Efficient numerical simulation of stochastic internal-wave-induced sound-speed perturbation fields

John A. Colosi, and Michael G. Brown

Citation: The Journal of the Acoustical Society of America **103**, 2232 (1998); doi: 10.1121/1.421381
View online: https://doi.org/10.1121/1.421381
View Table of Contents: https://asa.scitation.org/toc/jas/103/4
Published by the Acoustical Society of America

Efficient numerical simulation of stochastic internal-wave-induced sound-speed perturbation fields

John A. Colosi
Woods Hole Oceanographic Institution, Woods Hole, Massachusetts 02543

Michael G. Brown
Rosenstiel School of Marine and Atmospheric Science, University of Miami, 4600 Rickenbacker Causeway, Miami, Florida 33149

(Received 24 November 1996; accepted for publication 24 November 1997)

An efficient method is presented to numerically simulate stochastic internal-wave-induced sound-speed perturbation fields in deep ocean environments. The sound-speed perturbation field is represented as an internal-wave eigenfunction expansion in which WKB amplitude scaling and stretching of the depth coordinate are exploited. Individual realizations of the sound-speed perturbation field are constructed by evaluating a multidimensional fast Fourier transform of a complex-valued function whose modulus has a known simple form and whose phase is random. Approximations made are shown to be consistent with approximations built into the Garrett–Munk internal-wave spectrum, which is the starting point of this analysis. Both time-varying internal-wave fields in three space dimensions and frozen fields in a vertical plane are considered. © *1998 Acoustical Society of America*. [S0001-4966(98)02703-9]

PACS numbers: 43.30.Pc, 43.30.Ft [JHM]

INTRODUCTION

Internal-wave-induced sound-speed fluctuations are the dominant source of high-frequency variability of acoustic wave fields in the ocean.[1–3] Numerical simulations of acoustic wave fields in the presence of internal-wave-induced sound-speed perturbations have been shown to be extremely useful in the interpretation of measured wave fields[4–6] and for testing theoretical predictions.[7–11] A critical shortcoming of the numerical models that have been used previously to generate random realizations of internal-wave-induced sound-speed perturbation fields is their complexity; these models are as complicated and computationally intensive as the sound propagation models that are used to model the transmission of sound through the fields generated. The purpose of this paper is to describe a simple and efficient method to construct statistically realistic random realizations of internal-wave-induced sound-speed perturbation fields. We restrict our attention to deep ocean environments and assume that the statistics of the internal-wave field are described by the empirical Garrett–Munk (GM) spectrum.[12,13]

In addition to their complexity, previously used GM-based models of internal-wave-induced sound-speed perturbation fields have made compromises that violate the GM model. For example, Flatté and Tappert[2] only modeled internal waves which propagated in the direction of acoustic propagation and Colosi *et al.*[4] and Colosi and Flatté[10] generated several 16-km sections of statistically independent internal-wave fields which were patched together in range. Other approximations have been made.[6,7,11] This paper presents an efficient numerical technique for generating GM internal-wave-induced sound-speed perturbations without making the compromises of previous work.

Our new technique to construct sound-speed perturbation fields is based on an internal-wave eigenfunction expansion. The WKB amplitude and depth scaling are shown to lead to an extremely simple analytical description of the internal-wave vertical modes. Our use of WKB scaling is shown to be consistent with approximations already built into the GM spectrum. Thus, sound-speed perturbation fields produced with our simple technique have statistics which are consistent with predictions based on the GM spectrum. We consider both time-varying internal-wave fields in three space dimensions and frozen fields in a vertical plane. In both cases, the bulk of the computation required to construct a sound-speed perturbation field is the evaluation of a multidimensional fast Fourier transform.

I. INTERNAL-WAVE-INDUCED SOUND-SPEED FLUCTUATIONS

In this section we describe the mathematical formulation of our new method to construct sound-speed perturbation fields. Much of the material presented below is not new; our main contribution is the synthesis of this material into our new method. We include this material so that our presentation is self-contained. Our presentation of this background material is similar to the presentation in Ref. 11.

Internal-wave-induced sound-speed perturbations δc are proportional to internal-wave-induced vertical displacements ζ of a fluid parcel,[1,3]

$$\delta c=\left(\frac{\partial c}{\partial z}\right)_{\text{pot}}\zeta\approx c\left(\frac{\mu}{g}\right)N^2\zeta. \tag{1}$$

Here $(\partial c/\partial z)_{\text{pot}}$ is the potential sound-speed gradient, $\mu \approx 24.5$ is a dimensionless constant, $g=9.8\ \text{ms}^{-2}$ is the gravitational acceleration, c is sound speed, and N is buoyancy frequency. In practice, c in this equation can be treated as a constant, N can be treated as a slowly varying function of depth z [and perhaps also lateral position (x,y)], while δc and ζ are rapidly varying functions of x, y, z and t. Equation (1) provides a simple link between the statistics of $\zeta(x,y,z,t)$ and $\delta c(x,y,z,t)$.

Statistics of $\zeta(x,y,z,t)$ are described by the empirical GM internal-wave spectrum,[12,13]

$$F_{\zeta}(j,\omega)=\frac{2B^2E}{\pi M}\,\frac{N_0}{N}\,\frac{f}{\omega^3}\,(\omega^2-f^2)^{1/2}\,\frac{1}{(j^2+j_*^2)}\,. \qquad (2)$$

Here ω is the internal-wave angular frequency, j is the mode number, $j_*=3$ and $E=6.3\times10^{-5}$ are empirical dimensionless constants, f is the inertial frequency [$f=2\Omega\,\sin(\text{latitude})$ where $\Omega=2\pi/1$ day is the angular velocity of the earth], $B\approx1$ km is the thermocline depth scale, N_0 is the surface extrapolated buoyancy frequency, and $M=\Sigma_{j=1}^{\infty}(j^2+j_*^2)^{-1}\approx\frac{1}{2}j_*^{-2}(\pi j_*-1)$ is a normalization constant. It is often convenient to assume $N(z)=N_0\,\exp(z/B)$. More generally, we may define $N_0B=\int_{-h}^{0}N(z)dz$, where the ocean surface and bottom lie at $z=0$ and $z=-h$, respectively. The GM spectrum is normalized so that $\langle\zeta^2\rangle=\int_f^N d\omega\,\Sigma_{j=1}^{\infty}F_{\zeta}(j,\omega)=\frac{1}{2}B^2E\,(N_0/N)$, where the angular brackets denote average. It follows from the normalization that the product $(1/2)B^2E$ can be interpreted as ζ_0^2, the mean-square displacement at the depth at which $N=N_0$. The vertically integrated internal-wave potential energy density is $(\rho/2)\int_{-h}^{0}dz\,N^2\langle\zeta^2\rangle=(\rho/4)\,B^3N_0^2E$, where ρ is the density of sea water.

For some purposes it is convenient to replace the dependence of F_{ζ} on j or ω by dependence on horizontal wave number $k=(k_x^2+k_y^2)^{1/2}$ or vertical wave number m. These transformations require use of the dispersion relation:

$$\omega^2=N^2\,\frac{k^2}{k^2+m^2}+f^2\,\frac{m^2}{k^2+m^2}\approx\left(\frac{N_0B}{j\pi}\right)^2k^2+f^2\,. \qquad (3)$$

Both forms of the dispersion relation follow from a WKB analysis. The j-dependent form is a large j asymptotic result. The functions $F_{\zeta}(j,k_x,k_y)$ and $F_{\zeta}(j,k_x)$ are required below. Noting that $F_{\zeta}\,dj\,d\omega=F_{\zeta}\,dj\,dk(\partial\omega/\partial k)$ and using the approximate form of the dispersion relation [Eq. (3)] gives

$$F_{\zeta}(j,k)=\frac{2B^2E}{\pi M}\,\frac{N_0}{N}\,\frac{1}{(j^2+j_*^2)}\,\frac{k_jk^2}{(k^2+k_j^2)^2}\,, \qquad (4)$$

where $k_j=(f/N_0)(\pi j/B)$. When a change of variables is made, we normalize F_{ζ} so that the sum and/or integral of F_{ζ} over the domain of its arguments leaves $\langle\zeta^2\rangle$ unchanged. Because $2\pi\int_0^{\infty}dk\,kF(k)=\int_{-\infty}^{\infty}dk_x\int_{-\infty}^{\infty}dk_y\,F(\sqrt{k_x^2+k_y^2})$, we may write

$$F_{\zeta}(j,k_x,k_y)=\frac{B^2E}{\pi^2M}\,\frac{N_0}{N}\,\frac{1}{(j^2+j_*^2)}\,\frac{k_j\sqrt{k_x^2+k_y^2}}{(k_x^2+k_y^2+k_j^2)^2}\,. \qquad (5)$$

The reduction of $F_{\zeta}(j,k_x,k_y)$ to $F_{\zeta}(j,k_x)$ can be done analytically:

$$F_{\zeta}(j,k_x)=\int_{-\infty}^{\infty}dk_y\,F_{\zeta}(j,k_x,k_y)=\frac{I(j,k_x)}{j^2+j_*^2}\,\frac{B^2E}{\pi^2M}\,\frac{N_0}{N}\,, \qquad (6)$$

where

$$I(j,k_x)=\frac{k_j}{k_x^2+k_j^2}+\frac{1}{2}\,\frac{k_x^2}{(k_x^2+k_j^2)^{3/2}}\,\ln\left(\frac{\sqrt{k_x^2+k_j^2}+k_j}{\sqrt{k_x^2+k_j^2}-k_j}\right). \qquad (7)$$

This result was originally derived by Brill and Dozier.[14]

It is important to note that the GM spectrum is closely linked to WKB analysis. We have already used the WKB result (3) to derive $F_{\zeta}(j,k_x,k_y)$ and $F_{\zeta}(j,k_x)$. This usage is consistent with the manner in which the empirical GM spectral weights were chosen; to find the spectral weights which gave the best fit to a wide variety of internal-wave measurements (dropped, towed, fixed point, and combinations thereof). To the extent that these equations introduce a bias in the spectrum for small j and k, this bias has been compensated for by the choice of spectral weights. We emphasize this point because we make use of WKB scaling below; the approximations we make are entirely consistent with approximations already built into the GM spectrum.

For the purpose of generating random realizations of $\zeta(x,y,z,t)$ [and hence $\delta c(x,y,z,t)$] it is most useful to express ζ as a sum over internal-wave vertical modes in which the weights in the expansion are functions of j, k_x, and k_y. Let G_{ζ} denote F_{ζ} after renormalizing and omitting the depth dependence of the latter. The new normalization constant is chosen so that the vertically integrated internal-wave potential energy density is unchanged. These considerations give $G_{\zeta}=2BN_0NF_{\zeta}$, so

$$G_{\zeta}(j,k_x,k_y)=\frac{2B^3N_0^2E}{\pi^2M}\,\frac{1}{(j^2+j_*^2)}\,\frac{k_j\sqrt{k_x^2+k_y^2}}{(k_x^2+k_y^2+k_j^2)^2}\,. \qquad (8)$$

The desired modal expansion of ζ is then

$$\zeta(x,y,z,t)=\mathrm{Re}\left[\int\int dk_x\,dk_y\,\sum_j\,g(j,k_x,k_y)\times W_{jk}(z)e^{i(k_xx+k_yy-\omega_{jk}t)}\right], \qquad (9)$$

where each $g(j,k_x,k_y)$ is a complex Gaussian random variable with zero mean and variance $\langle g(j,k_x,k_y)g^*(j',k_x',k_y')\rangle=G_{\zeta}(j,k_x,k_y)\,\delta_{jj'}\,\delta(k_x-k_x')\,\delta(k_y-k_y')$. Construction of the modes $W_{jk}(z)$ will be discussed below. These are orthonormal, $\int_{-h}^{0}dz(N^2(z)-f^2)W_{jk}(z)W_{j'k}(z)=\delta_{jj'}$, from which it follows that $\int dzN^2(z)W_{jk}^2(z)\approx1$. The mean-square displacement is $\langle\zeta^2\rangle=\frac{1}{2}\int\int dk_x\,dk_y\,\Sigma_jG_{\zeta}(j,k_x,k_y)W_{jk}^2(z)$, and the vertically integrated internal-wave potential energy density is $(\rho/2)\int dz\,N^2(z)\langle\zeta^2\rangle\approx(\rho/4)\int\int dk_x\,dk_y\,\Sigma_jG_{\zeta}(j,k_x,k_y)=(\rho/4)\,B^3N_0^2E$, consistent with the result found earlier.

To model sound propagation in a frozen (not evolving in time) vertical slice (range and depth) of the ocean, the double integral over k_x and k_y in (9) can be reduced to a single integral. This is partially justified by the horizontal isotropy of the internal-wave field; we may, without loss of generality, take the propagation plane to coincide with the $y=0$ plane. To treat this problem we require

$$G_{\zeta}(j,k_x)=\int_{-\infty}^{\infty}dk_y\,G_{\zeta}(j,k_x,k_y)=\frac{I(j,k_x)}{j^2+j_*^2}\,\frac{2B^3N_0^2E}{\pi^2M}\,, \qquad (10)$$

where $I(j,k_x)$ is defined above [Eq. (7)]. The frozen (we set $t=0$ for convenience) vertical slice representation of ζ is then

$$\zeta(x,z)=\mathrm{Re}\left[\int dk_x\,\sum_j\,g(j,k_x)W_{jk_x}(z)e^{ik_xx}\right], \qquad (11)$$

where each $g(j,k_x)$ is a complex Gaussian random variable with zero mean and variance $\langle g(j,k_x) g^*(j',k_x')\rangle = G_\zeta(j,k_x)\delta_{jj'}\delta(k_x-k_x')$. Note that k_y is set equal to zero when the modes $W_{jk_x}(z)$ are constructed. The mean-square displacement is now $\langle\zeta^2\rangle = \frac{1}{2}\int dk_x\, \Sigma_j G_\zeta(j,k_x) W^2_{jk_x}(z)$, and the vertically integrated internal-wave potential energy density is $(\rho/2)\int dz\, N^2(z)\langle\zeta^2\rangle \approx (\rho/4)\int dk_x\, \Sigma_j G_\zeta(j,k_x) = (\rho/4)\, B^3 N_0^2 E$, consistent with results found previously.

We turn our attention now to the difficult part of evaluating Eqs. (9) and (11). This is the problem of constructing the internal-wave modes, $W_{jk}(z)$, which satisfy

$$\frac{d^2W}{dz^2} + k^2\,\frac{N^2(z)-\omega^2}{\omega^2-f^2}\,W(z) = 0 \tag{12}$$

subject to the boundary conditions $W(0)=W(-h)=0$, and the related problem of finding ω_{jk}. {Note, however, that an assumed form of ω_{jk} [Eq. (3)] has already been used.} Consistent with the observation that WKB scaling is already built into (9) and (11), we now invoke WKB scaling of both the modal amplitudes and the depth coordinate by introducing

$$V(z) = (N(z)/N_0)^{1/2} W(z) \tag{13}$$

and

$$\xi(z) = \frac{1}{N_0 B}\int_{-h}^{z} N(z')\,dz'. \tag{14}$$

Similar transformations are routinely used in the analysis of field observations of internal waves.[15–17] It follows from the definition of Eqs. (13) and (14), and the observation that $N>0$, that ξ increases monotonically from 0 at $z=-h$ to 1 at $z=0$. Equation (12) written in terms of $V(z)$ is

$$\frac{3}{4N^2}\left(\frac{dN}{dz}\right)^2 V(z) - \frac{1}{2N}\frac{d^2N}{dz^2}V(z) - \frac{1}{N}\frac{dN}{dz}\frac{dV}{dz} + \frac{d^2V}{dz^2} + k^2\,\frac{N^2(z)-\omega^2}{\omega^2-f^2}\,V(z) = 0. \tag{15}$$

It will be shown below that the first two terms in this equation can be neglected. Transforming the remaining terms from z to ξ and noting that $N^2-\omega^2 \approx N^2$, consistent with GM approximations, gives

$$\frac{d^2V}{d\xi^2} + k^2B^2\,\frac{N_0^2}{\omega^2-f^2}\,V(\xi) = 0 \tag{16}$$

subject to the boundary conditions $V(\xi=0)=V(\xi=1)=0$. Solutions are

$$V_j(\xi) = (1/N_0)(2/B)^{1/2}\sin(j\pi\xi) \tag{17}$$

with

$$kBN_0/\sqrt{\omega^2-f^2} = j\pi. \tag{18}$$

Here j is a positive integer and the modes are normalized so that the modal orthogonality condition with $N^2-f^2\approx N^2$ is satisfied. Note that Eq. (18) is identical to Eq. (3) which was used to derive $G_\zeta(j,k)$.

To assess the validity of neglecting the first two terms in Eq. (15), it is insightful to assume $N(z)=N_0\exp(z/B)$. Substituting this N into (15) and making use of Eqs. (17) and (18) leads to the conclusion that the first two terms in (15) are negligible when $(2j\pi)^2 \gg (N_0/N)^2$. For more general buoyancy frequency profiles, our WKB treatment will be valid wherever the local vertical wavelength of mode j is small compared to the local vertical length scale of N. This condition may be violated for small j. Recall, however, our earlier comments about the GM spectral weights; to the extent that the use of large j asymptotic results bias the spectrum, this bias has been compensated for by the choice of the spectral weights. Again we emphasize that our approximations are consistent with approximations already built into the GM spectrum. Note also that in the deep ocean (where N/N_0 is small) errors in ζ associated with violation of the condition $(2j\pi)^2\gg(N_0/N)^2$ should give negligible errors in δc because δc is proportional to $N^2\zeta$.

The preceding discussion provides a complete mathematical description of our new technique to generate random realizations of ζ [or, using Eq. (1), δc]. We now summarize, rewriting the relevant equations in a form which is convenient for numerical purposes. For the time-dependent field in three space dimensions

$$\zeta(x,y,z,t) = \mathrm{Re}\left[\frac{2B}{\pi}\left(\frac{E}{M}\right)^{1/2}\left(\frac{N_0}{N(z)}\right)^{1/2}(\Delta k_x)^{1/2}(\Delta k_y)^{1/2} \times \sum_j \frac{k_j^{1/2}\sin(j\pi\xi(z))}{(j^2+j_*^2)^{1/2}}\sum_{k_x}\sum_{k_y}\frac{(k_x^2+k_y^2)^{1/4}}{k_x^2+k_y^2+k_j^2} \times e^{i\phi(j,k_x,k_y)}e^{i(k_x x+k_y y-\omega_{jk}t)}\right]. \tag{19}$$

Here ω_{jk} is defined by Eq. (18), Δk_x and Δk_y are the step sizes used in the integrals over k_x and k_y, and $\phi(j,k_x,k_y)$ is a delta-correlated random variable with a uniform distribution between 0 and 2π. For the frozen vertical slice problem,

$$\zeta(x,z) = \mathrm{Re}\left[\frac{2B}{\pi}\left(\frac{E}{M}\right)^{1/2}\left(\frac{N_0}{N(z)}\right)^{1/2}(\Delta k_x)^{1/2} \times \sum_j \frac{\sin(j\pi\xi(z))}{(j^2+j_*^2)^{1/2}}\sum_{k_x}(I(j,k_x))^{1/2}e^{i\phi(j,k_x)}e^{ik_x x}\right], \tag{20}$$

where $I(j,k_x)$ is defined by Eq. (7). It should be noted that (19) and (20) are consistent with the GM spectral densities $F_\zeta(j,k_x,k_y)$ [Eq. (5)] and $F_\zeta(j,k_x)$ [Eq. (6)] presented above.

To numerically demonstrate the use of our new description of ζ we have computed $\delta c(x,z)$ using Eqs. (19) and (20) for an exponentially stratified ocean, $N(z)=N_0\exp(z/B)$ with $N_0=2\pi/10$ min and $B=1$ km, whose depth is 5 km. [For this simple case $z=B\ln(\xi+e^{-5})$.] Simulations, produced by evaluating Eqs. (1) and (19), are shown in Figs. 1 and 2. Figure 1 shows plots of $(N/N_0)^{-3/2}\delta c$ versus range at selected depths, at a fixed time. Figure 2 shows plots of $(N/N_0)^{-3/2}\delta c$ versus time at selected fixed locations. For these simulations we used $512\times512(k_x,k_y)$ values with $2\pi/100\ \mathrm{km}\leqslant|k_x|,\ |k_y|\leqslant 2\pi/1\ \mathrm{km}$, and $j_{\max}=50$. Our numerical estimates of the following statistical properties of δc and $\partial\delta c/\partial z$ have been found to be consistent with predictions[1,3,11] based on the GM spectrum: (i) $(\delta c)_{\mathrm{rms}}$ scales

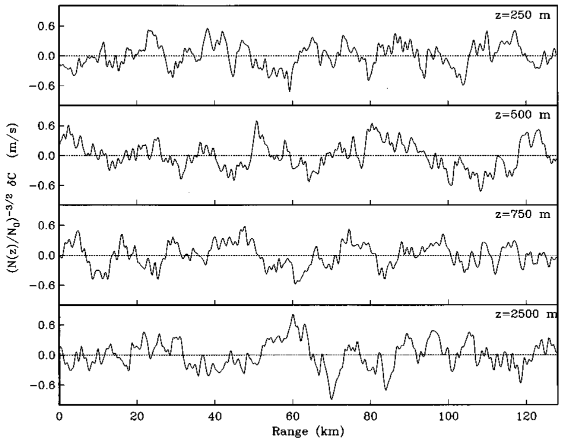

FIG. 1. Plots of $(N/N_0)^{-3/2}\delta c$ versus range at selected depths, at a fixed time, computed using Eqs. (1) and (31).

in depth like $N^{3/2}$; (ii) $(\partial \delta c/\partial z)_{\mathrm{rms}}$ scales in depth like $N^{5/2}$; (iii) the horizontal and vertical correlation lengths of δc are approximately $(\pi/8)\times(B/j_*)(N_0/f)/\ln[(N/f)-1/2]$ and $(B/(\pi j_*-1))\times(N_0/N)$, respectively; and (iv) the horizontal and vertical correlation lengths of $\partial \delta c/\partial z$ are approximately $\pi/(k_x)_{\max}$ and $(B/j_{\max})(N_0/N)$, respectively.

II. SUMMARY

In this paper we have described an extremely simple and efficient technique to simulate internal-wave-induced sound-speed perturbation fields. Our analysis is based on the empirical GM internal-wave spectrum and thus should not be expected to apply at very high latitudes, very low latitudes, or in coastal regions. Use of WKB scaling in our analysis is entirely consistent with approximations already built into the GM spectrum. In addition to simplicity and efficiency, the new method has several advantages over previously used techniques: (i) it is true to the GM spectrum (the technique used by Colosi *et al.*[4] and Colosi and Flatté[10] distorts the horizontal wave-number spectrum predicted by GM); (ii) both the surface and bottom boundary conditions are satisfied exactly (the technique used by Brown and Viechnicki[11] assumes an infinitely deep ocean); (iii) no restrictive assumptions about $N(z)$ (e.g., monotonicity, which is assumed by Brown and Viechnicki[11]) are required; (iv) lateral variability of N and/or the ocean depth can easily be treated (Colosi *et al.*,[4] Dozier and Tappert,[7,8] Colosi and Flatté,[10] and Brown and Viechnicki[11] do not address this problem but Wolfson *et al.*[6] does); (v) three-dimensional δc fields can be generated; and (vi) time-dependent δc fields can be generated.

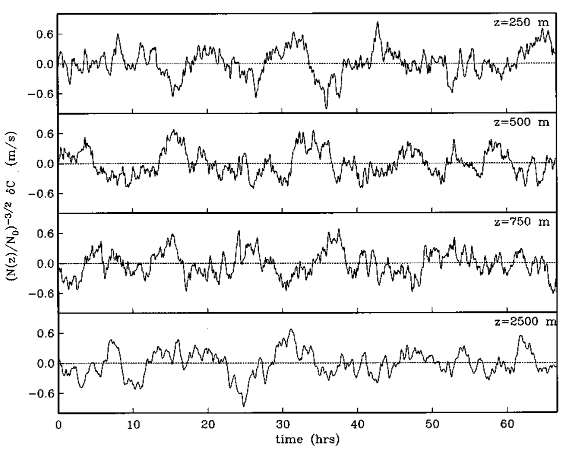

FIG. 2. Plots of $(N/N_0)^{-3/2}\delta c$ versus time at selected fixed locations, computed using Eqs. (1) and (31). The increasing smoothness of the time series plotted as depth increases (especially visible at 2500 m) is consistent with the GM prediction that the correlation time for δc at a fixed location is approximately $(\pi/(2fN))^{1/2}$.

ACKNOWLEDGMENTS

We thank W. Munk, F. Tappert, and M. Wolfson for the benefit of our discussions on internal-wave-induced sound speed fluctuations. This work was funded by the Office of Naval Research Grant Nos. N00014-97-1-0046 and N00014-97-1-0068. This is Woods Hole Oceanographic Institution contribution number 9374.

[1] W. H. Munk and F. Zachariasen, ''Sound propagation through a fluctuating stratified ocean: Theory and observation,'' J. Acoust. Soc. Am. **59**, 818–838 (1976).

[2] S. M. Flatté and F. D. Tappert, ''Calculation of the effects of internal waves on oceanic sound transmission,'' J. Acoust. Soc. Am. **58**, 1151–1159 (1975).

[3] S. Flatté, R. Dashen, W. Munk, K. Watson, and F. Zachariasen, *Sound Transmission through a Fluctuating Ocean* (Cambridge U.P., Cambridge, 1979).

[4] J. A. Colosi, S. M. Flatté, and C. Bracher, ''Internal-wave effects on 1000-km oceanic acoustic pulse propagation: Simulation and comparison to experiment,'' J. Acoust. Soc. Am. **96**, 452–468 (1994).

[5] P. F. Worcester *et al.*, ''A test of basin-scale acoustic thermometry using a large-aperture vertical array at 3250-km range in the eastern North Pacific Ocean,'' submitted to J. Acoust. Soc. Am. (1997).

[6] M. A. Wolfson and J. Spiesberger, ''Full wave simulations of the forward scattering of sound in a structured ocean: A comparison with observations,'' submitted to J. Acoust. Soc. Am. (1997).

[7] L. B. Dozier and F. D. Tappert, ''Statistics of normal mode amplitudes in a random ocean. I. Theory,'' J. Acoust. Soc. Am. **63**, 353–365 (1978).

[8] L. B. Dozier and F. D. Tappert, ''Statistics of normal mode amplitudes in a random ocean. II. Computations,'' J. Acoust. Soc. Am. **64**, 533–547 (1978).

[9] S. M. Flatté and G. Rovner, ''Path-integral expressions for fluctuations in acoustic transmission in the ocean waveguide,'' Proceedings of the 1997 Aha Hulikoá Winter Workshop (1997).

[10] J. A. Colosi and S. M. Flatté, ''Mode coupling by internal waves for multi-megameter acoustic propagation in the ocean,'' J. Acoust. Soc. Am. **100**, 3607–3620 (1996).

[11] M. G. Brown and J. Viechnicki, ''Stochastic ray theory for long-range sound propagation in deep ocean environments,'' J. Acoust. Soc. Am. (to be published).

[12] C. Garrett and W. Munk, ''Space-time scales of ocean internal waves,'' Geophys. Fluid Dyn. **2**, 225–264 (1972).

[13] W. Munk, ''Internal waves and small-scale processes,'' in *The Evolution of Physical Oceanography*, edited by C. Wunsch and B. Warren (MIT, Cambridge, 1981), pp. 264–291.

[14] M. H. Brill and L. B. Dozier, ''Exact transition from two- to one-dimensional internal wave power spectra,'' J. Acoust. Soc. Am. **77**, 1248–1249 (1985).

[15] J. T. Bell, ''Processing vertical internal-wave spectra,'' J. Phys. Oceanogr. **4**, 669–670 (1974).

[16] R. Pinkel, ''Doppler sonar observations of internal waves: The wave-number-frequency spectrum,'' J. Phys. Oceanogr. **14**, 1249–1270 (1984).

[17] T. F. Duda and C. S. Cox, ''Vertical wavenumber spectra of velocity and shear at small internal-wave scales,'' J. Geophys. Res. **94**, 939–950 (1989).